

Supporting Information

Two Carboxyethyltin Functionalized Polyoxometalates for Assembly on Carbon Nanotubes as Efficient Counter Electrode Materials in Dye-Sensitized Solar Cells

Xiao-Jing Sang,^{‡b} Jian-Sheng Li,^{‡b} Lan-Cui Zhang,^{*a} Zai-Ming Zhu,^a Wei-Lin Chen,^{*b} Yang-Guang Li,^b Zhong-Min Su,^b En-Bo Wang^{*b}

^a School of Chemistry and Chemical Engineering, Liaoning Normal University, Dalian 116029.

^b Key Laboratory of Polyoxometalate Science of Ministry of Education, Faculty of Chemistry, Northeast Normal University, Changchun, Jilin 130024, People's Republic of China

CONTENTS:

I. Experimental Section

II. Supplementary Structure Figures

III. Supplementary Physical and Chemical Characterizations

IV. Tables

I. Experimental Section

1. Materials and Methods

$\text{Na}_{12}[\text{Cu}_4(\text{H}_2\text{O})_2(\text{GeW}_9\text{O}_{34})_2] \cdot 38\text{H}_2\text{O}$ (abbreviated as GeW_9Cu_4) and $\text{Na}_{12}[\text{Co}_4(\text{H}_2\text{O})_2(\text{GeW}_9\text{O}_{34})_2] \cdot 35\text{H}_2\text{O}$ (abbreviated as GeW_9Co_4) were synthesized according to the reported methods^{S1} and characterized by FTIR. SWNT (JCST-90-2-10) was purchased from JCNANO. All other chemical reagents were commercially purchased and used without further purification. Elemental analyses for C, H and N were performed on a Vario Elcube elemental analyzer. The elemental analyses of Ge, Cu, Co, Sn and W were analyzed on a Plasma-Spec-II ICP atomic emission spectrometer. IR spectra were recorded using KBr pellets on a Bruker AXS TENSOR-27 FTIR spectrometer in the range of 4000–400 cm^{-1} . TG analyses were performed on a Pyris Diamond TG-DTA thermal analyzer at a heating rate of 10 $^\circ\text{C min}^{-1}$ from 30 to 1000 $^\circ\text{C}$. X-ray powder diffraction data was collected on a Bruker AXS D8 Advance diffractometer using Cu $K\alpha$ radiation ($\lambda = 1.5418 \text{ \AA}$) in the 2θ range of 5–60 $^\circ$ with a step size of 0.02 $^\circ$. Cyclic voltammograms were recorded using a three electrode system comprising of glassy carbon electrode as the working electrode, a Pt wire as the counter electrode and Ag/AgCl reference electrode. NaAc/HAc buffer solution with pH 6.5 was used as the supporting electrolyte. XPS was performed on F-doped SnO_2 glass using an ESCALAB-MKII photoelectronic spectrometer with an Mg $K\alpha$ (1253.6eV) achromatic X-ray source. The morphology and nanostructure of the samples were characterized with High resolution transmission electron microscope (HRTEM) (JEOL-2100F) at an acceleration voltage of 200 kV. All photoelectrochemical experiments were performed on a Model CS350 electrochemistry station (CH Instruments, Wuhan CorrTest Instrument Corporation, PRC) at room temperature equipped with Xenon lamp as the light source.

2. Synthesis

Synthesis of $\text{GeW}_9\text{-Cu-SnR}$: GeW_9Cu_4 (1.16 g, 0.2 mmol) was dissolved in 15 mL water, and to which a 10 mL aqueous solution of $\text{Cl}_3\text{SnCH}_2\text{CH}_2\text{COOCH}_3$ (0.24 g, 0.77 mmol) was added dropwise with stirring. The resulting solution was stirred at 80 $^\circ\text{C}$ for about 2 h. After cooling to room temperature, several drops of 1 mol L^{-1} $[\text{C}(\text{NH}_2)_3]\text{Cl}$ and 3.86 g KCl were added to the mixture, to provide a light green precipitate. The crude product was recrystallized by dissolution in 15 mL water. Light green columnar-shaped single crystals were harvested by slow evaporation for one week (yield 41% based on Ge). Elemental analysis calc. for $\text{C}_{16}\text{H}_{84}\text{Ge}_2\text{Cu}_2\text{N}_{30}\text{O}_{79}\text{Sn}_2\text{W}_{18}$ (%): C, 3.32; H, 1.46; Ge, 2.51; Cu, 2.20; N, 7.27; Sn,

4.11;W, 57.24. Found (%): C, 3.36; H, 1.50; Ge, 2.50; Cu, 2.18; N, 7.24; Sn, 4.12; W, 57.25. IR (solid KBr pellet ν/cm^{-1}): 3427(s), 3177(w), 2917(w), 2859(w), 1653(m), 1214(w), 959(m), 866(m), 774(s), 734(s), 518(w), 467(w).

Synthesis of GeW₉-Co-SnR: The preparation process was similar to that for GeW₉-Cu-SnR, except that GeW₉Co₄ was used. The product was isolated in the form of purple columnar-shaped single crystals after one week. Yield: 25% based on Ge. Elemental analysis calc. for C₁₆H₈₆Ge₂Co₂N₃₀O₈₀Sn₂W₁₈ (%): C, 3.32; H, 1.50; Ge, 2.51; Co, 2.04; N, 7.26; Sn, 4.10; W, 57.15. Found (%): C, 3.31; H, 1.45; Ge, 2.52; Co, 2.03; N, 7.24; Sn, 4.10; W, 57.18. IR (solid KBr pellet ν/cm^{-1}): 3413(s), 2912(w), 2851(w), 1661(s), 1404(m), 948(m), 873(s), 782(s), 737(s), 524(w), 463(w).

3. Crystallography

X-ray diffraction data were collected on a Bruker Smart APEXII X-diffractometer equipped with graphite-monochromated Mo K α radiation ($\lambda = 0.71073 \text{ \AA}$). An empirical absorption correction was applied using the SADABS program. The structures were solved by direct methods and refined by the full-matrix least-squares fitting on F^2 using the SHELXTL-97 package.^{S2} Cell parameters were obtained by the global refinement of the positions of all collected reflections. All the non-hydrogen atoms were refined anisotropically. Hydrogen atoms on C and N atoms were added in calculated positions. Crystal data and structure refinement parameters of GeW₉-Cu-SnR and GeW₉-Co-SnR are listed in Table S1. Selected bond lengths and angles are listed in Table S2 and S3, and hydrogen bonds are given in Table S4 and S5. CCDC-1012852 (GeW₉-Cu-SnR), CCDC-1012926 (GeW₉-Co-SnR) contain the supplementary crystallographic data for this paper. These data can be obtained free of charge from The Cambridge Crystallographic Data Centre via www.ccdc.cam.ac.uk/data-request/cif.

4. Preparation of CEs

Preparation of SWNT electrode: Firstly, SWNT paste was obtained with a similar method documented in the literature.^{S3} Briefly, SWNT powder was mixed and grounded with certain amount of glacial acetic acid, ethanol, terpineol and ethylcellulose, followed by evaporating for concentration. Then screen-printing technique was used to coat the SWNT paste on the FTO conductive glass which was ultrasonic cleaned with surfactant, isopropanol and ethanol respectively. This screen-printing procedure was repeated for four times to control the electrode thickness. Finally the SWNT coated electrode was sintered at 300 °C for 15 min before use.

Preparation of POMs-modified SWNT electrode: Cyclic voltammetry method was employed to deposit POMs on the SWNT electrode, in which the SWNT electrode was used as the working electrode, a Pt wire was used as the counter electrode and Ag/AgCl electrode was used as the reference electrode. The electrolyte solution was constituted of 0.5 mmol L⁻¹ POMs in NaAc/ HAc buffer solution with the pH of 6.5. The voltage range were from 0.2 V to -1.2 V at the scanning rate of 100 mV/s. Besides **GeW₉-Cu-SnR** and **GeW₉-Co-SnR**, GeW₉Cu₄ and Na₁₀[GeW₉O₃₄]·18H₂O (abbreviated as GeW₉) were adopted for comparison.

Preparation of SnR-modified SWNT electrode: Specifically, the SnR-modified SWNT electrodes (denoted as SWNT/ SnR) were fabricated by electrodeposition, which employed the three-electrode system consisting of bare SWNT electrode as the working electrode, a Pt wire as the counter electrode and Ag/AgCl electrode as the reference electrode. The electrolyte solution was constituted of 0.1 mmol L⁻¹ SnR in 0.1 mol L⁻¹ Na₂SO₄ solution. The voltage range were from 0.2 V to -1.2 V at the scanning rate of 100 mV/s with scanning segment of 60.

5. Solar Cell Fabrication

Cells using N719 sensitizer with I₃⁻/I⁻-based mediator: The TiO₂ paste was prepared according to the similar method in the literature.^{S3} After ball-milling for 1 h, the obtained paste was further treated at 90 °C for about 20 min under stirring to reaching the suitable concentration for screen printing. Then a 12 μm thick TiO₂ film (P25, Degussa, Germany, Figure S3) was prepared by screen-printing the TiO₂ paste on the FTO glass which had been ultrasonic cleaned with surfactant, isopropanol and ethanol. Four layers of paste was deposited on the FTO glass to control the thickness of the TiO₂ working electrode. Layers were then sintered at 325 °C for 5 min, 375 °C for 5 min, and 450 °C for 30 min. Subsequently, the resulting films were post-treated in 40 mmol L⁻¹ TiCl₄ solution for 30 min at 70 °C and calcined in air at 450 °C for 30 min again. When cooled to 80 °C, the film was immersed in 0.25 mg/ mL N719 (Solaronix SA, Switzerland) ethanol solution for 24h. After washing off the unanchored dye, the DSSC was fabricated by sandwiching a dye-sensitized TiO₂ film and a CE. Finally, an electrolyte solution consisting of 0.1 mol L⁻¹ LiI, 0.05 mol L⁻¹ I₂, 0.6 mol L⁻¹ 1,2-dimethyl-3-propylimidazolium iodide, 0.5 mol L⁻¹ 4-tert-butylpyridine in 3-methoxypropionitrile, was introduced between the electrodes by the capillary action.

Cells using Z907 sensitizer with I₃⁻/I⁻-based mediator: The FTO glass that had been ultrasonic cleaned with surfactant, isopropanol and ethanol was pre-treated by immersing into a 40 mmol L⁻¹ TiCl₄ aqueous solution at 70 °C for 30 min.

TiO₂ photoanode was fabricated by coating the TiO₂ paste^{S3} (P25, Degussa, Germany) onto the processed FTO glass through screen-printing technique. Different from iodine-based cells, two layers of paste was deposited on the FTO glass to control the thickness of the TiO₂ working electrode. Layers were then sintered at 325 °C for 5 min, 375 °C for 5 min, and 450 °C for 30 min. Subsequently, the resulting films were post-treated in 40 mmol L⁻¹ TiCl₄ solution for 30 min at 70 °C and calcined in air at 450 °C for 30 min again. When cooled to 80 °C, the film was immersed in 5×10⁻⁴ mol L⁻¹ Z907 (Solaronix SA, Switzerland) ethanol solution for 24h. After washing off the unanchored dye, the DSSC was fabricated by sandwiching a dye-sensitized TiO₂ film and a CE. Finally, the electrolyte solution (OPV-AN-C) containing Co(III/II) was introduced between the electrodes by the capillary action.

Firstly, TiO₂ photoanodes were prepared by coating TiO₂ paste on the FTO conductive glass which was ultrasonic cleaned with surfactant, isopropanol and ethanol through screen printing. After sintering at 450 °C for 30 min, the resulting films were post-treated in 40 mmol L⁻¹ TiCl₄ solution 30 min at 70 °C and calcined in air at 450 °C for 30 min again. When cooled to 80 °C, the film was immersed in N719 ethanol solution for 24h. Subsequently the dye-covered electrodes were covered with the obtained various SWNT-based electrodes as counter electrodes. Finally, an electrolyte solution, which was composed of 0.1 mol L⁻¹ LiI, 0.05 mol L⁻¹ I₂, 0.6 mol L⁻¹ 1,2-dimethyl-3-propylimidazolium iodide, 0.5 mol L⁻¹ 4-tert-butylpyridine in 3-methoxypropionitrile, was introduced between the electrodes by the capillary action.

II. Crystal Structure Figures

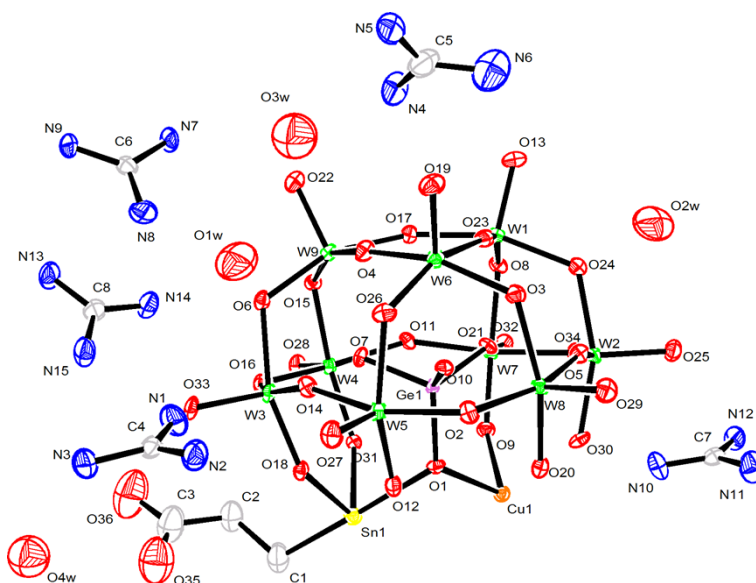


Figure S1. ORTEP drawing of the polyoxoanion of GeW₉-Cu-SnR with thermal ellipsoids at 30%

probability

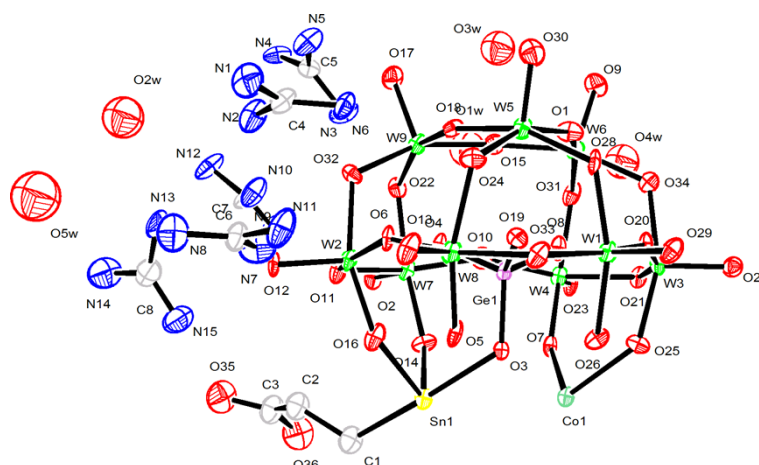


Figure S2. ORTEP drawing of the polyoxoanion of GeW_9 -Co-SnR with thermal ellipsoids at 30% probability

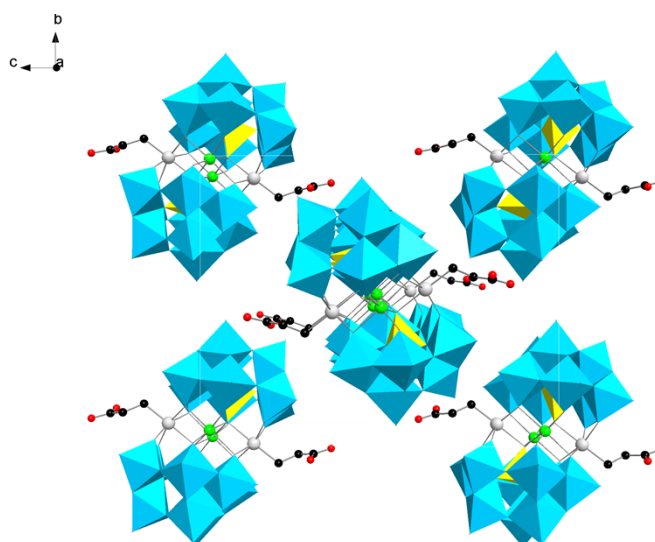


Figure S3. Polyhedral and ball-and-stick view of the 3D supramolecular framework of GeW_9 -Cu-SnR. Cyan, W; Yellow, Ge; Green, Cu; Gray, Sn; Dark, C; Red, O. All H atoms, the isolated $[C(NH_2)_3]^+$ and water molecules reside in the interspaces are omitted for clarity

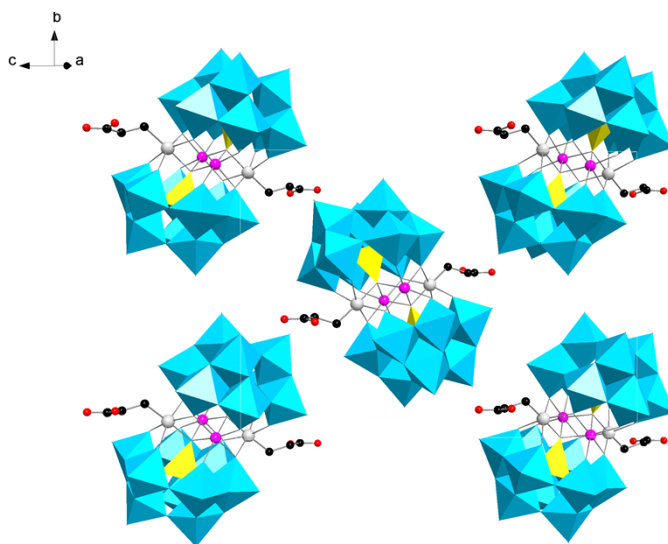


Figure S4. Polyhedral and ball-and-stick view of the 2D supramolecular framework of **GeW₉-Co-SnR**. Cyan, W; Yellow, Ge; Magenta, Co; Gray, Sn; Dark, C; Red, O. All H atoms, the isolated [C(NH₂)₃]⁺ and water molecules reside in the interspaces are omitted for clarity

III. Supplementary Physical and Chemical Characterizations

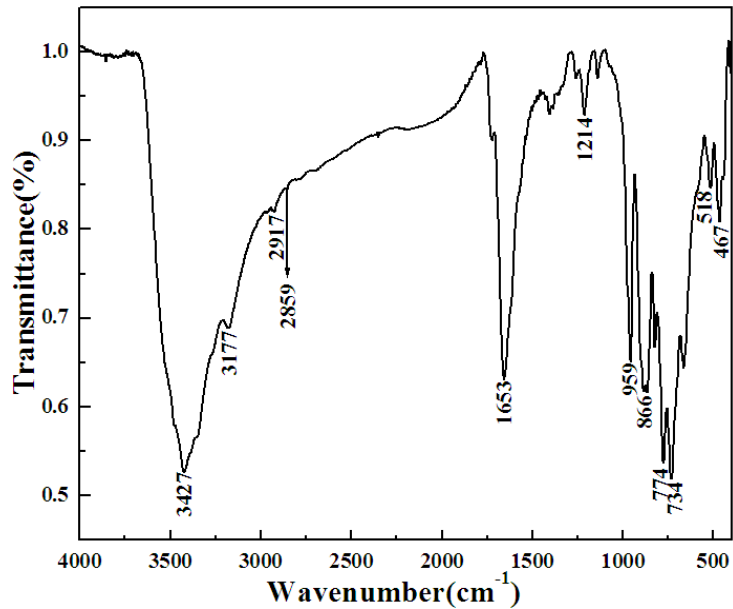


Figure S5. FTIR spectrum for **GeW₉-Cu-SnR**

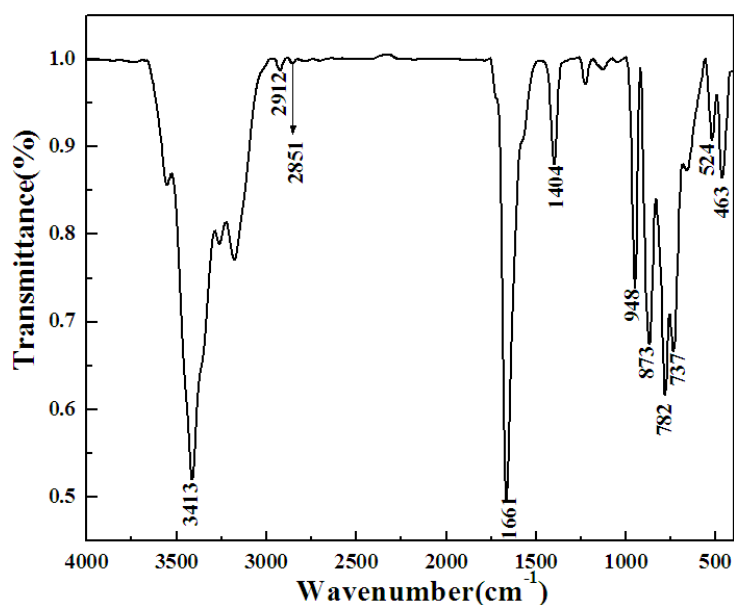


Figure S6. FTIR spectrum for **GeW₉-Co-SnR**

The characteristic peaks of FTIR spectra for **GeW₉-Cu-SnR** and **GeW₉-Co-SnR** are similar. As shown in Figures S5 and S6, the wide bands at 3427/3413 cm^{-1} are attributed to $\nu(\text{O-H})$ vibration of coordinate and crystal water. The peaks at 2917/2912 and 2859/2851 cm^{-1} are attributed to the organic group $-\text{CH}_2$. The peaks at 1653/1661 cm^{-1} are assigned to $\nu_{\text{as}}(\text{COO}^-)$ and $\nu_{\text{s}}(\text{COO}^-)$ vibration. The characteristic vibrations of $\nu(\text{W-O}_d)$, $\nu(\text{W-O}_b\text{-W, Sn})$, $\nu(\text{Ge-O}_a)$ and $\nu(\text{W-O}_c\text{-W})$ of POMs appear at 959/948, 866/873, 774/782 and 734/737 cm^{-1} respectively (O_d , terminal O atoms; O_b , O_c , bridging O atoms). The peaks at 518/524 and 467/463 cm^{-1} are ascribed to the antisymmetric and symmetric vibration of Sn-C bonds.

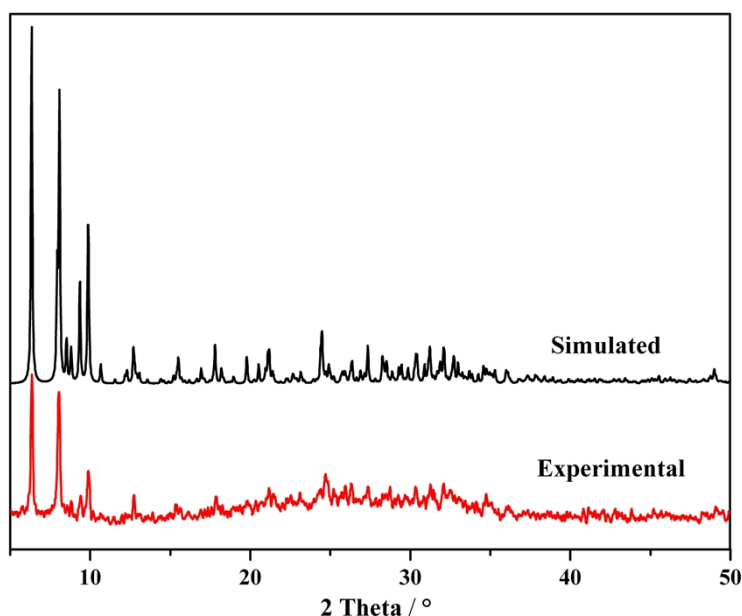


Figure S7. (a) The simulated and (b) experimental XRPD patterns of **GeW₉-Cu-SnR**

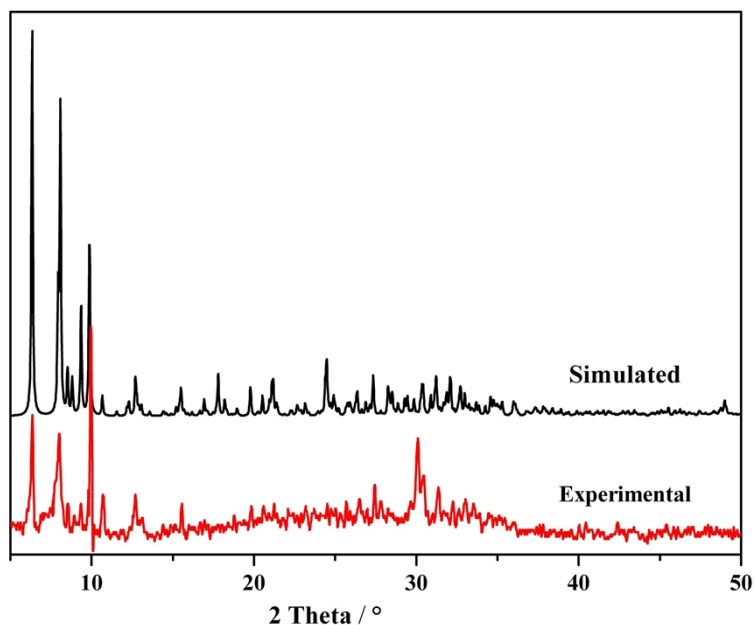


Figure S8. (a) The simulated and (b) experimental XRPD patterns of **GeW₉-Co-SnR**

Figure S7 and S8 show the powder XRD patterns of **GeW₉-Cu-SnR** and **GeW₉-Co-SnR** (red line) and their simulated PXRD patterns (dark line). As can be seen, the main peaks of experimental results are in good agreement with simulated ones for both **GeW₉-Cu-SnR** and **GeW₉-Co-SnR**, confirming that the products are pure phases. The differences in reflection intensity are probably due to preferred orientation in the powder samples.

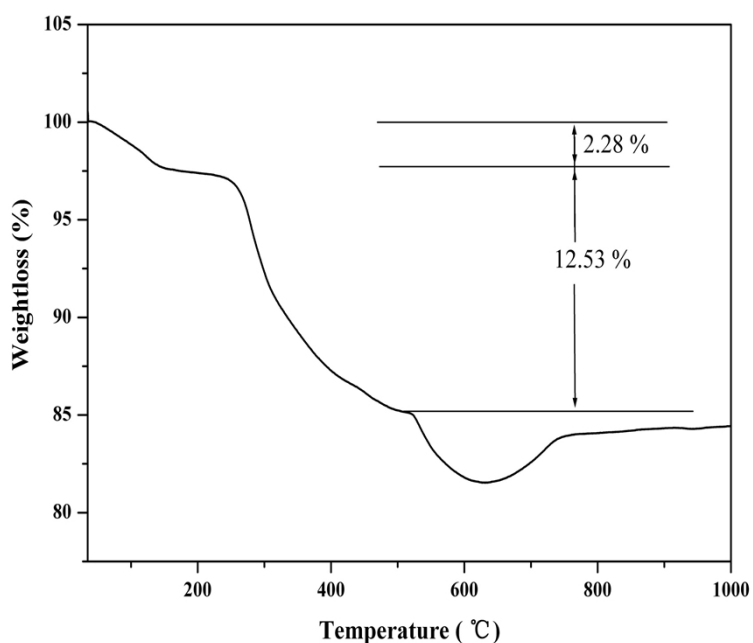


Figure S9. TG curve of **GeW₉-Cu-SnR**

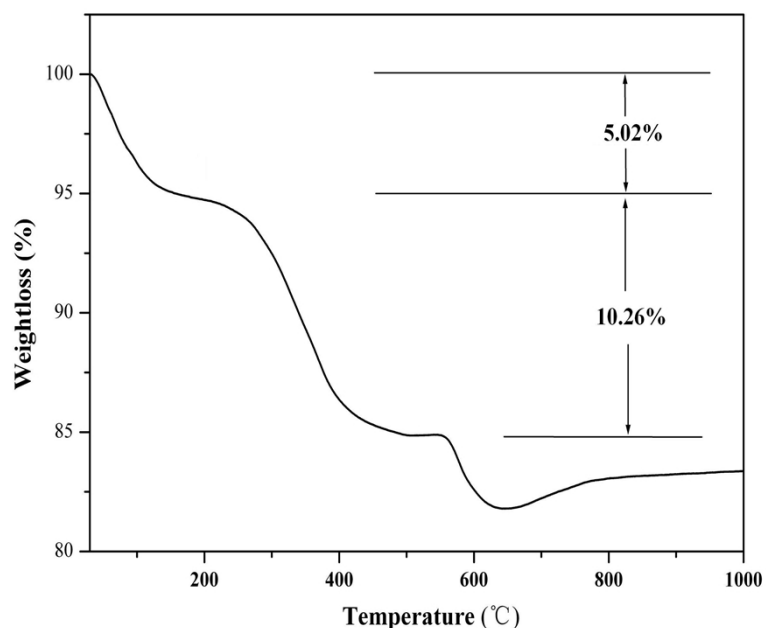


Figure S10. TG curve of **GeW₉-Co-SnR**

The TG curve of **GeW₉-Cu-SnR** in Figure S9 shows the first weight loss step of 2.28% (calc. 2.18%) in the range of 35-143 °C, which corresponds to the loss of all water molecules. The second weightloss of 12.53% (calc. 12.91%) in the range of 142-521 °C was corresponding to the loss of ten C(NH₂)₃ groups, two H and two C₃H₄O₂ groups. The TG curve of **GeW₉-Co-SnR** in Figure S10 was slight different from that of **GeW₉-Cu-SnR**, from which the first weightloss of 5.02% (calc. 4.98%) in the range of 30-161 °C was attributed to the loss of all water molecules, two C₃H₄O₂ groups and two H and the second weightloss of 10.26% (calc. 10.40%) was due to the loss of ten C(NH₂)₃ groups.

For both **GeW₉-Cu-SnR** and **GeW₉-Co-SnR**, further temperature increment lead to continuous weightloss, indicating that the skeleton of POMs decomposed. The TG curves have slightly rise after 632 °C for **GeW₉-Cu-SnR** and 650 °C for **GeW₉-Co-SnR**. This phenomenon also occurs in other similar compounds, which may be caused by the oxidation of tin in air atmosphere.

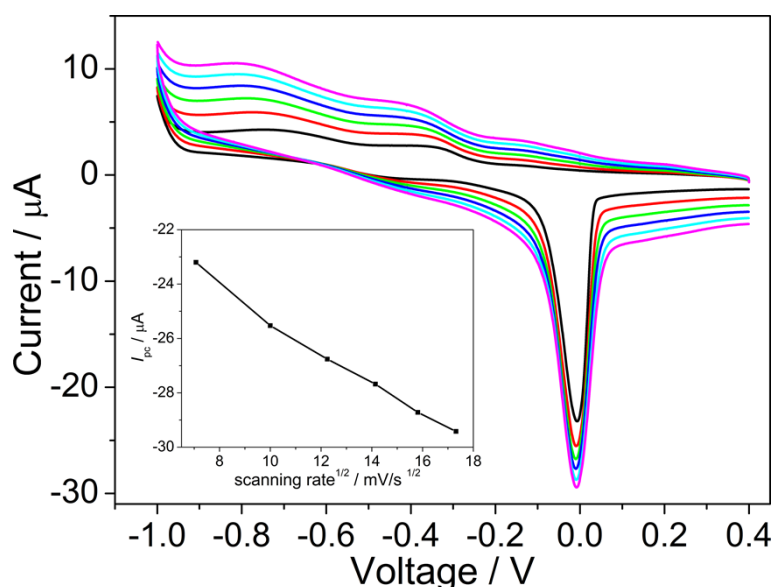


Figure S11 The cyclic voltammograms of **GeW₉-Cu-SnR** in NaAc/ HAc solution with pH 6.5 at different scanning rates: 50 mV/s (dark line); 100 mV/s (red line); 150 mV/s (green line); 200 mV/s (blue line); 250 mV/s (cyan line); 300 mV/s (magenta line). The inset is the plot of peak current versus square root of scanning rate

The electrochemical property of **GeW₉-Cu-SnR** was investigated by measuring its CV curve in the NaAc/ HAc buffer solution with pH of 6.5. As shown in Figure S11, the reduction peaks at -0.35 V and -0.73 V are attributed to the reduction processes of W centers in the polyanions. The oxidation peak located at -0.005V is assigned to the redox process of Cu²⁺/ Cu⁰. Furthermore, according to the linear relationship between the anodic peak current and the square root of the scan rate in the inset of Figure S11, this electrochemical process is diffusion controlled.

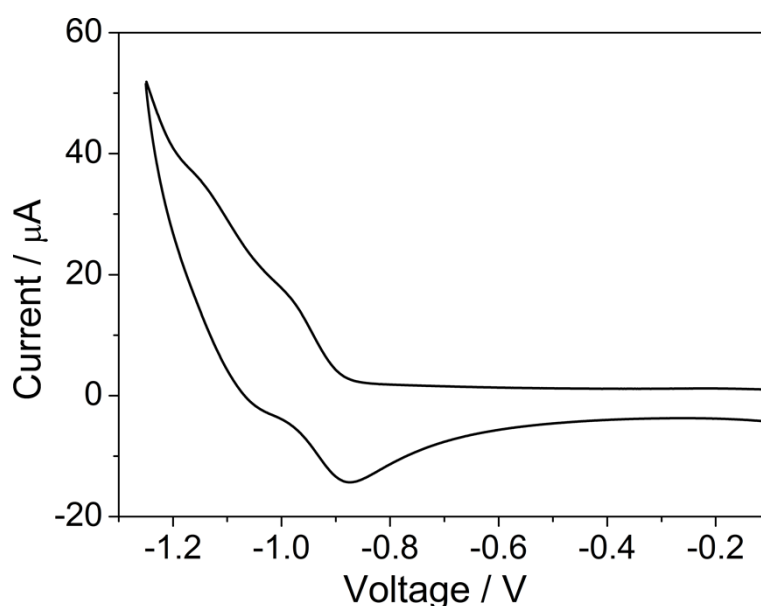


Figure S12 The cyclic voltammogram of **GeW₉-Co-SnR** in NaAc/ HAc solution with pH 6.5 at

200 mV/s

According to the CV curve in Figure S12, there are two successive reduction peaks at -0.98 V and -1.13 V for **GeW₉-Co-SnR**, corresponding to their oxidation peaks located at -0.88 V and -1.05 V, which are ascribed to the redox processes of W centers in the polyanions.

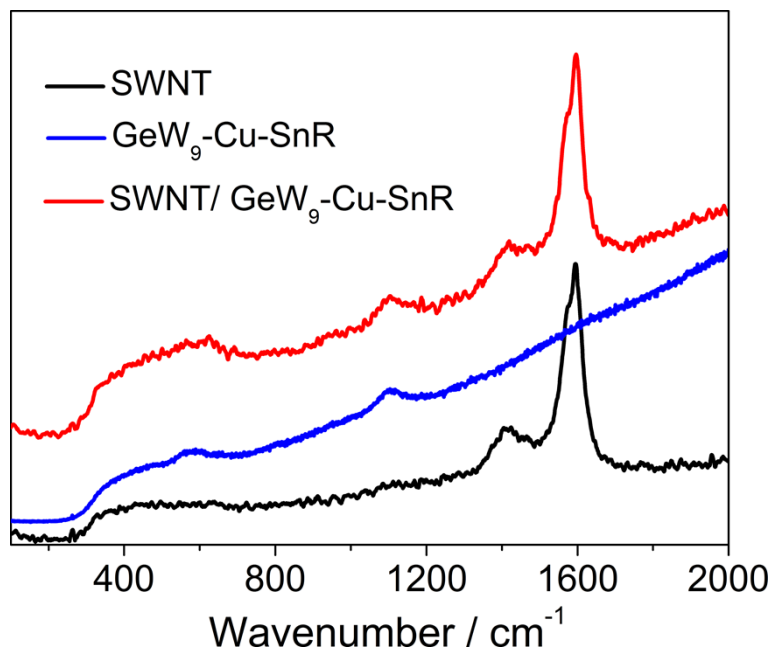


Figure S13 Raman spectra of SWNT electrode (dark line); **GeW₉-Cu-SnR** powder (blue line) and **GeW₉-Cu-SnR**-modified SWNT electrode (red line)

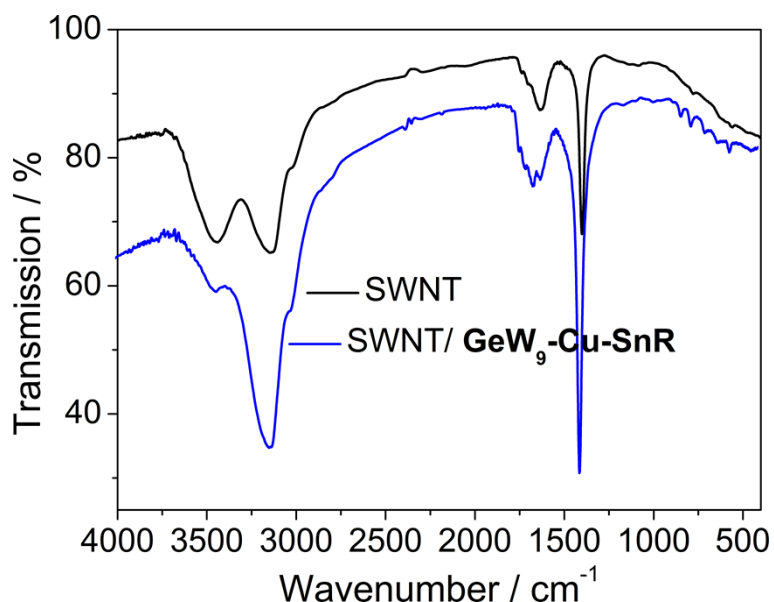


Figure S14 FTIR spectrum of SWNT (dark line) and SWNT/ **GeW₉-Cu-SnR** (blue line)

Comparing the FTIR spectrum in Figure S14, SWNT/ **GeW₉-Cu-SnR** display the additional peaks at 988, 880, 833 and 777 cm⁻¹ relative to bare SWNT, which could be attributed to the characteristic vibrations of $\nu(\text{W}-\text{O}_d)$, $\nu(\text{W}-\text{O}_b-\text{W}, \text{Sn})$, $\nu(\text{Ge}-\text{O}_a)$ and $\nu(\text{W}-\text{O}_c-\text{W})$ of POMs;

meantime, the peaks at 563 cm^{-1} and 441 cm^{-1} could be ascribed to the antisymmetric and symmetric vibration of Sn–C bonds. This result indicated that **GeW₉-Cu-SnR** could retain its complete structure after incorporation with SWNT.

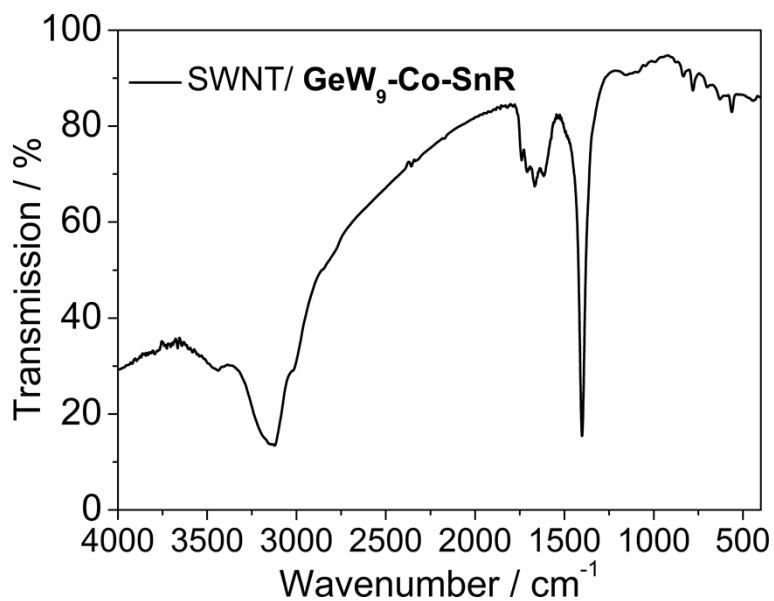


Figure S15 FTIR spectrum of SWNT/ **GeW₉-Co-SnR**

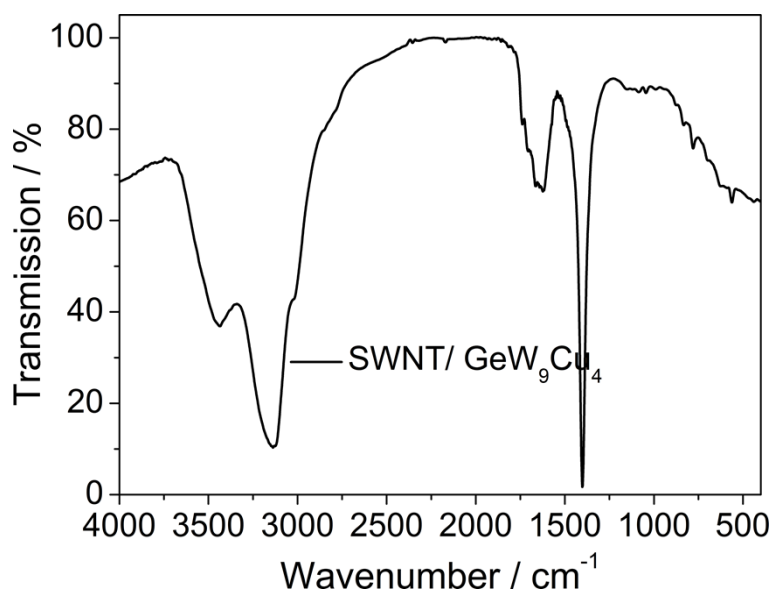


Figure S16 FTIR spectrum of SWNT/ GeW₉Cu₄

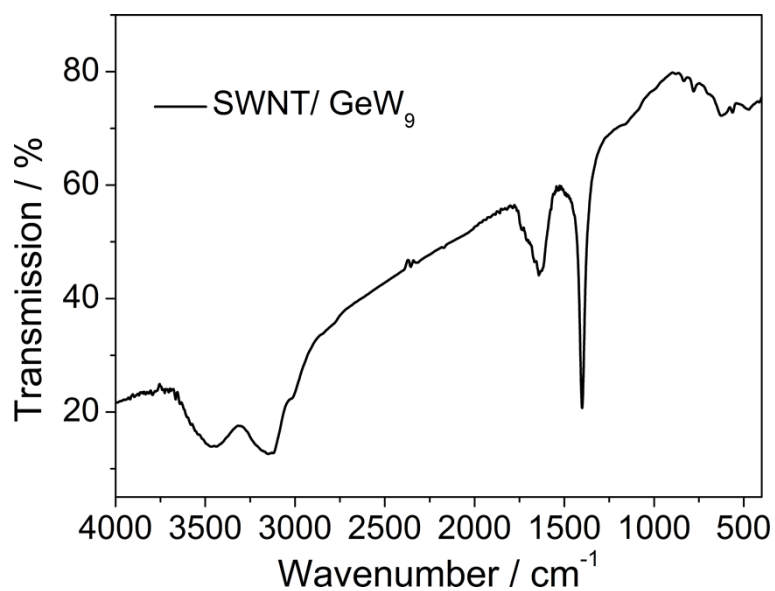


Figure S17 FTIR spectrum of SWNT/ GeW₉

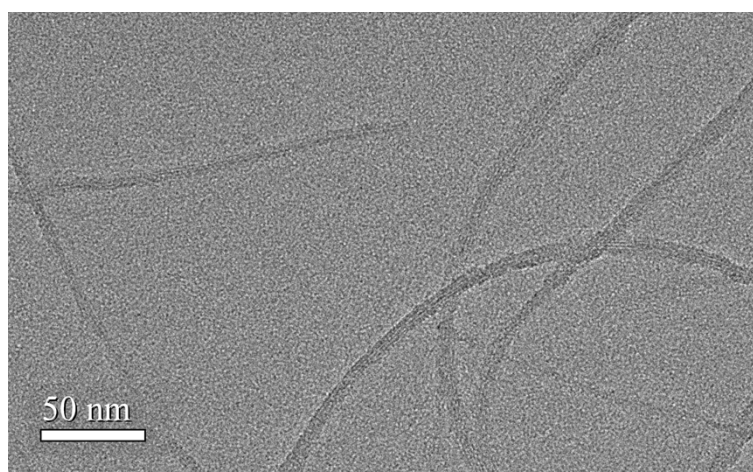


Figure S18 HRTEM image of SWNT. SWNT possess the relatively smooth surface with the diameter of 5-10 nm

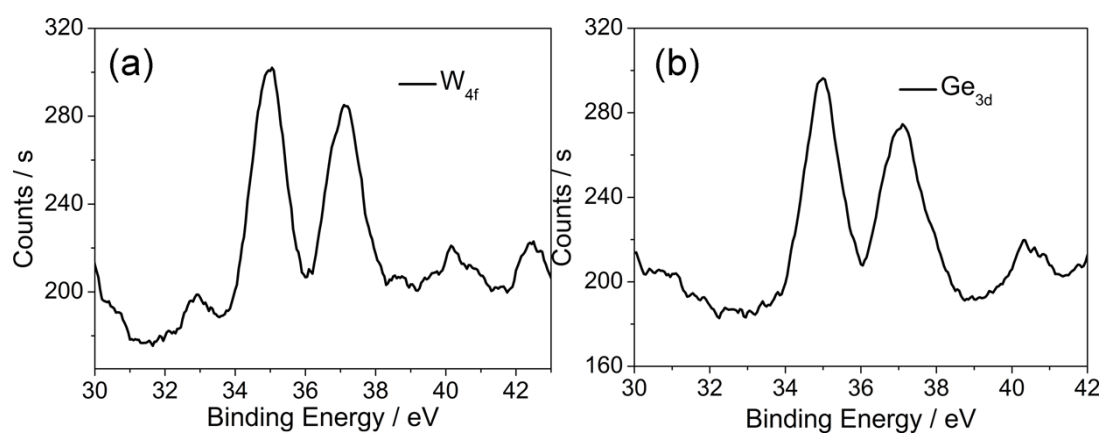


Figure S19 XPS spectra of SWNT/ GeW₉-Co-SnR for (a) W and (b) Ge

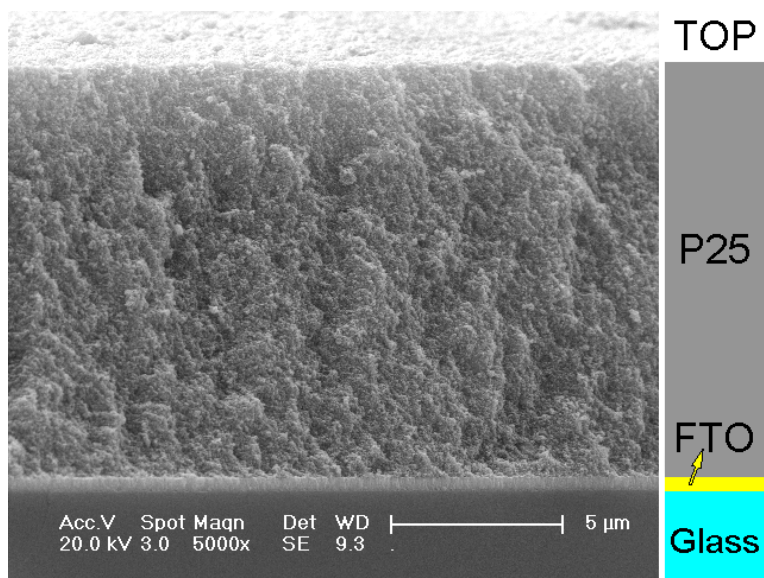


Figure S20. The cross-sectional SEM image of the TiO₂ film fabricated by screen-printing

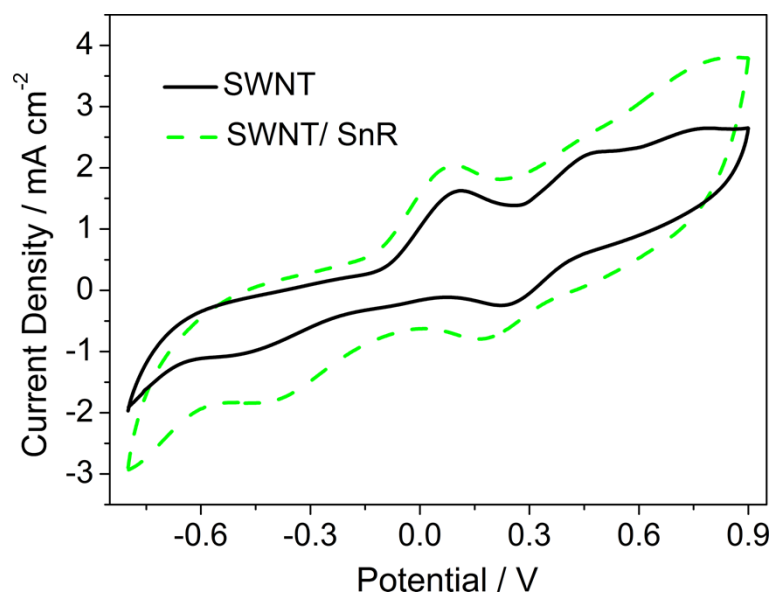


Figure S21 Cyclic voltammograms for the I⁻/I₃⁻ redox reaction of SWNT and SWNT/ SnR CE

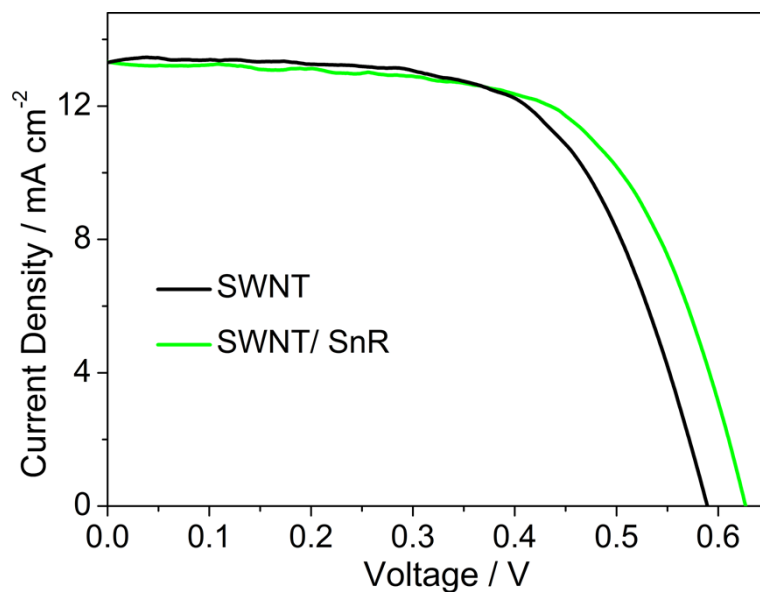


Figure S22 *J-V* curves of DSSCs using SWNT

and SWNT/ SnR CE under one sun illumination (AM 1.5G, 100 mW cm⁻²)

The CV curves for the I⁻/I₃⁻ redox reaction of SWNT and SWNT/ SnR electrode are shown in Figure S21. As can be seen, modifying SWNT with SnR could decrease the E_{pp} on the left that corresponds to oxidation and reduction of I⁻/I₃⁻ from 538 mV to 469 mV. Especially, it could significantly enhance the cathodic peak current involving the reduction of I₃⁻, indicating that SnR could improve the electrocatalytic activity toward triiodide reduction as the modifiers of SWNT electrode. Furthermore, the DSSCs with SWNT/ SnR as the CE were fabricated to assess its electrocatalytic performance. Figure S22 shows the $J-V$ curves, which displays that modification with SnR could obviously improve the open-circuit voltage and fill factor, with conversion efficiency increased by 7.04% (from 4.97% to 5.32%). Similarly, five set of parallel experiments were carried out, and an average data of these results and the standard deviation derived from the average value are summarized in Table S7. The $J-V$ curve in Figure S22 represents the set of data mostly close to the average value. To sum up, the enhancement of the electro-catalytic activities after the carboxyethyltin modification could be attributed to the additional catalytic site by the organotin portion. The synergistic effect of POMs and organotin fragment could contribute to the final remarkable electro-catalytic activities of POM-organotin derivatives.

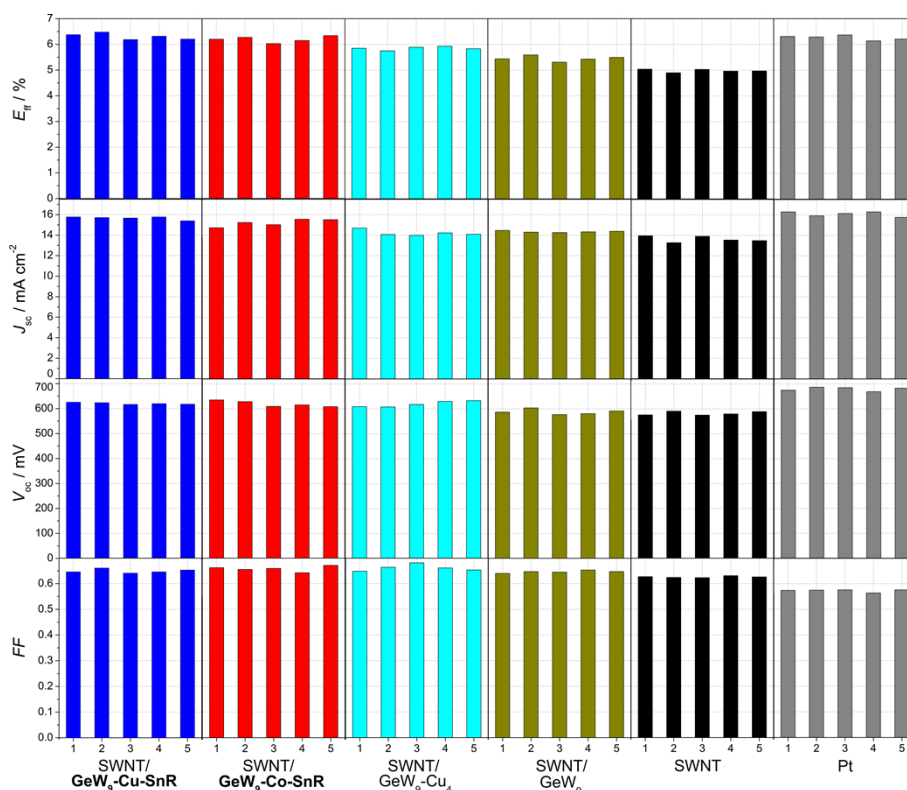


Figure S23. The photovoltaic characteristics for five sets of DSSCs using various CEs with N719 sensitizer and I₃⁻/I⁻-based mediator

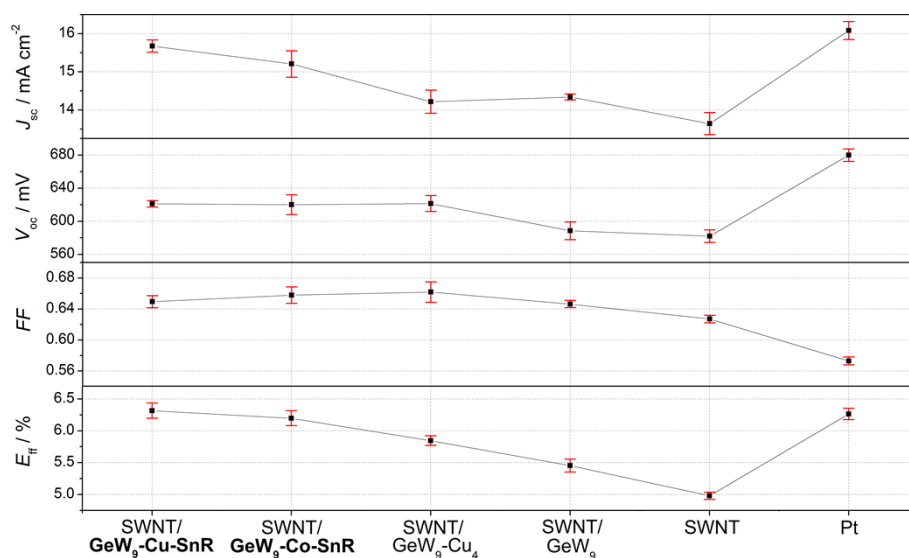


Figure S24. The error bar for J_{sc} , V_{oc} , FF and E_{ff} of the DSSCs based on various CEs with N719 sensitizer and I_3^-/I^- -based mediator

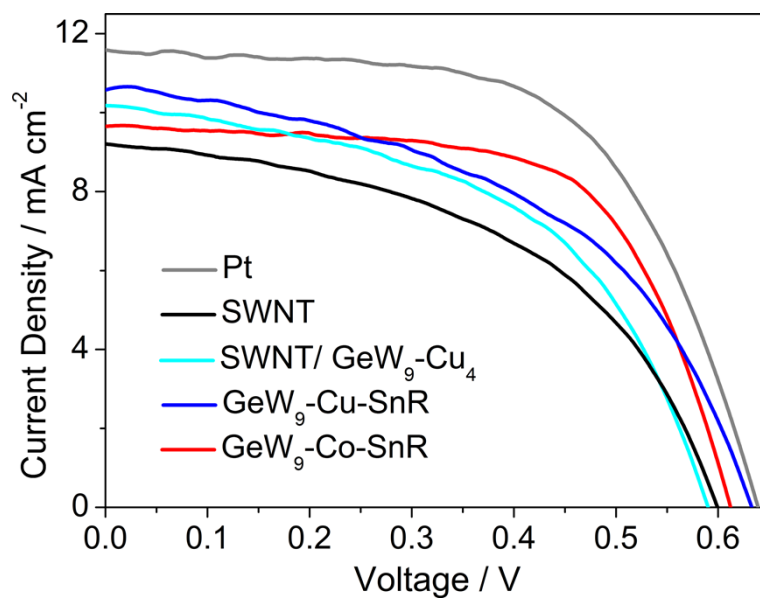


Figure S25. J - V curves of the DSSCs based on various CEs with Z907 sensitizer and a Co(III/II)-based mediator, measured under one sun illumination (AM 1.5G, 100 mW cm⁻²)

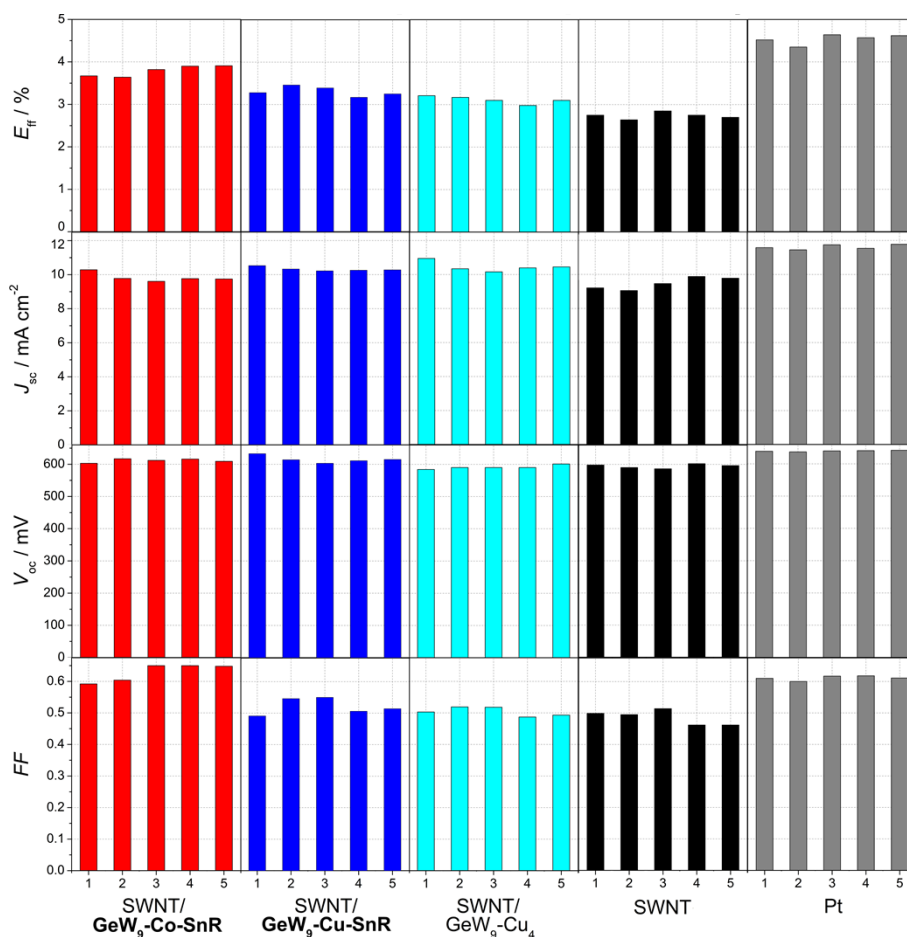


Figure S26. The photovoltaic characteristics for five sets of DSSCs using various CEs with Z907 sensitizer and a Co(III/II)-based mediator

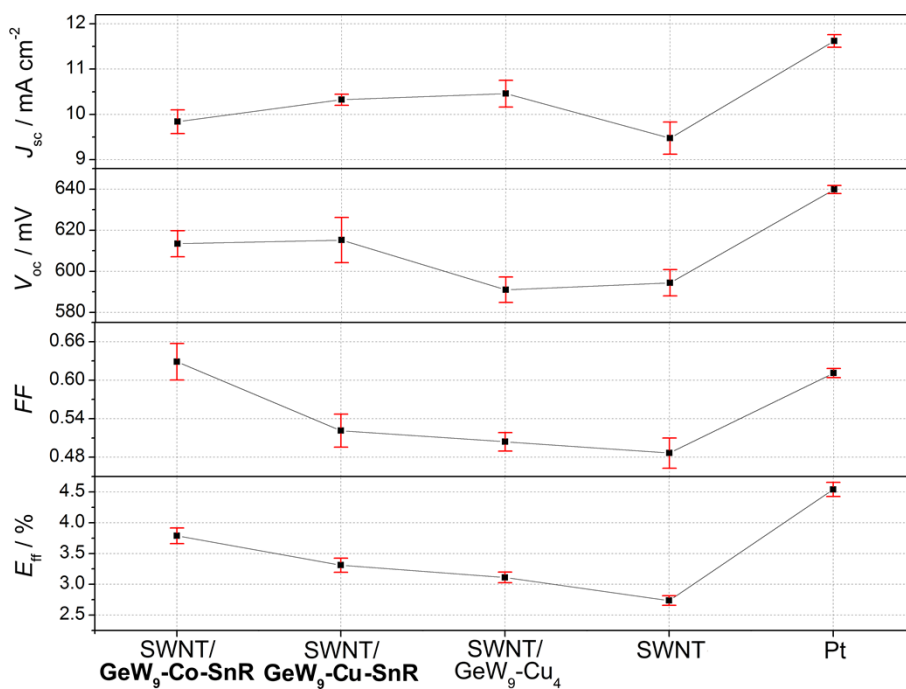


Figure S27. The error bar for J_{sc} , V_{oc} , FF and E_{ff} of the DSSCs based on various CEs with Z907 sensitizer and a Co(III/II)-based mediator

Figure S25 compares the photocurrent-voltage (J - V) characteristics of the DSSCs based on various CEs using Z907 as the sensitizer with a Co(III/II)-based mediator, and the photovoltaic parameters of the corresponding DSSCs are summarized in Table S13. To assess the reproducibility of the DSSCs with various CEs, five sets of parallel experiments were carried out for each kind of CE, and an average data of these results and the standard deviation derived from the average value are summarized in Tables S14-S18. The photovoltaic characteristics for the cells and corresponding error bar are shown in Figure S26-S27. The J - V curves in Figure S25 represents the set of data mostly close to the average value. As can be concluded, the DSSC using SWNT as the CE generates a E_{ff} of 2.75%, with short-circuit current density (J_{sc}) of 9.21 mA cm⁻², open-circuit voltage (V_{oc}) of 598 mV and fill factor (FF) of 0.499. Remarkably, the DSSC with Pt as the CE shows superior performance to ones with SWNT-based CE, which presents a E_{ff} of 4.52%, with J_{sc} of 11.58 mA cm⁻², V_{oc} of 639 mV and FF of 0.610. However, the performance of DSSCs could be significantly enhanced by employing the composite CEs SWNT/ **GeW₉-Co-SnR** or SWNT/ **GeW₉-Cu-SnR**. Especially, the FF of DSSC with SWNT/ **GeW₉-Co-SnR** CE was increased by 30.3% with E_{ff} increased by 38.9% compared with DSSC that used SWNT-only as the CE. These results demonstrated that the two POM-carboxyethyltin derivatives could also improve the catalytic activity of SWNT electrode toward reduction of the Co(III) component. Furthermore, the precursor of **GeW₉-Cu-SnR**, GeW₉-Cu₄ could improve the J_{sc} and E_{ff} of DSSC to some extent; on the contrary, GeW₉ did not show the positive effect which gave E_{ff} of only 2.34% (data not shown), indicating that the transition metal ions may contribute to the catalytic activity.

IV. Tables

Table S1. Crystal and Refinement Data for **GeW₉-Cu-SnR** and **GeW₉-Co-SnR**

Compound	GeW₉-Cu-SnR	GeW₉-Co-SnR
Formula	C ₁₆ H ₈₄ N ₃₀ Cu ₂ Sn ₂ Ge ₂ W ₁₈ O ₇₉	C ₁₆ H ₈₆ N ₃₀ Co ₂ Sn ₂ Ge ₂ W ₁₈ O ₈₀
Formula weight /g mol ⁻¹	5780.07	5788.77
Wavelength /Å	0.71073	0.71073
T /K	296(2)	296(2)
Crystal size /mm	0.09 × 0.08 × 0.05	0.09 × 0.07 × 0.06
Crystal system	Monoclinic	Monoclinic
Space group	$P2_1/n$	$P2_1/c$
a /Å	12.2645(18)	12.430(8)
b /Å	18.000(3)	18.096(12)
c /Å	22.276(3)	25.144(13)
β /°	94.009(2)	115.63(2)

$V/\text{\AA}^3$	4905.6(13)	5099(5)
Z	2	2
$D_c/\text{Mg m}^{-3}$	3.913	3.770
μ/mm^{-1}	22.649	21.698
$F(000)$	5152	5162
R_{int}	0.0369	0.0954
$R_1(I > 2\sigma(I))^a$	0.0292	0.0688
wR_2 (all data) ^a	0.0704	0.1942
Goodness-of-fit on F^2	1.035	1.066

$$^aR_1 = \sum||F_0|-|F_c||/\sum|F_0|; wR_2 = \sum[w(F_0^2-F_c^2)^2]/\sum[w(F_0^2)^2]^{1/2}$$

Table S2. Selected bond lengths (Å) and angles (°) for **GeW₉-Cu-SnR**

Bond	Length (Å)	Bond	Length (Å)	Bond	Length (Å)
W1-O13	1.727(7)	W5-O12	1.787(7)	W9-O15	1.910(6)
W1-O8	1.870(7)	W5-O14	1.950(7)	W9-O4	1.918(7)
W1-O17	1.921(6)	W5-O2	1.976(6)	W9-O17	1.932(6)
W1-O23	1.923(6)	W5-O26	2.024(7)	W9-O7	2.390(7)
W1-O24	1.925(7)	W5-O10	2.277(6)	Sn1-O31	2.042(6)
W1-O21	2.444(6)	W6-O19	1.716(7)	Sn1-O18	2.059(6)
W2-O25	1.724(7)	W6-O26	1.887(7)	Sn1-O30#1	2.074(6)
W2-O30	1.872(7)	W6-O3	1.917(7)	Sn1-O20#1	2.090(6)
W2-O34	1.902(6)	W6-O4	1.919(7)	Sn1-C1	2.153(14)
W2-O5	1.937(7)	W6-O23	1.923(6)	Sn1-O1	2.340(6)
W2-O24	1.972(7)	W6-O10	2.425(6)	Ge1-O21	1.746(6)
W2-O21	2.335(6)	W7-O32	1.723(7)	Ge1-O10	1.747(6)
W3-O33	1.727(6)	W7-O9	1.800(7)	Ge1-O7	1.758(6)
W3-O18	1.841(7)	W7-O11	1.927(6)	Ge1-O1	1.777(6)
W3-O14	1.909(6)	W7-O34	1.995(6)	Cu1-O12#1	1.941(7)
W3-O16	1.958(6)	W7-O8	2.041(7)	Cu1-O9	1.964(7)
W3-O6	1.991(7)	W7-O21	2.268(6)	Cu1-O1	2.055(6)
W3-O7	2.299(6)	W8-O29	1.713(7)	Cu1-O1#1	2.101(6)
W4-O28	1.718(7)	W8-O20	1.870(7)	Cu1-O20#1	2.332(7)
W4-O31	1.829(6)	W8-O2	1.923(6)	Cu1-O30	2.334(7)

W4-O11	1.941(6)	W8-O5	1.933(6)	C1-C2	1.524(18)
W4-O16	1.947(6)	W8-O3	1.979(7)	C2-C3	1.48(2)
W4-O15	1.995(7)	W8-O10	2.327(6)	C3-O35	1.23(2)
W4-O7	2.308(6)	W9-O22	1.715(7)	C3-O36	1.31(2)
W5-O27	1.729(7)	W9-O6	1.904(6)		
Bond	Angle(°)	Bond	Angle(°)	Bond	Angle(°)
O13-W1-O21	169.9(3)	O27-W5-O10	168.1(3)	O22-W9-O7	171.0(3)
O8-W1-O23	156.2(3)	O14-W5-O2	158.7(3)	O15-W9-O4	157.2(3)
O23-W1-O24	86.9(3)	O14-W5-O26	85.3(3)	O15-W9-O17	87.3(3)
O8-W1-O24	90.0(3)	O2-W5-O26	82.5(3)	O4-W9-O17	85.8(3)
O25-W2-O21	168.3(3)	O19-W6-O10	169.4(3)	O10-Ge1-O1	113.3(3)
O34-W2-O5	157.7(3)	O3-W6-O4	158.3(3)	O21-Ge1-O7	107.8(3)
O34-W2-O24	87.2(3)	O3-W6-O23	86.5(3)	O21-Ge1-O10	105.5(3)
O5-W2-O24	86.1(3)	O4-W6-O23	84.7(3)	O7-Ge1-O1	110.4(3)
O33-W3-O7	168.8(3)	O32-W7-O21	166.9(3)	C1-Sn1-O1	178.6(4)
O14-W3-O16	158.6(3)	O11-W7-O34	158.8(3)	O31-Sn1-C1	96.4(4)
O14-W3-O6	89.3(3)	O11-W7-O8	87.3(3)	O31-Sn1-O1	82.4(2)
O16-W3-O6	82.1(3)	O34-W7-O8	81.7(3)	O18-Sn1-O30#1	89.4(3)
O28-W4-O7	169.9(3)	O29-W8-O10	166.8(3)	O20#1-Cu1-O30	171.7(2)
O11-W4-O16	157.7(3)	O2-W8-O5	158.1(3)	O9-Cu1-O1	94.3(3)
O11-W4-O15	86.8(3)	O2-W8-O3	86.4(3)	O9-Cu1-O20#1	93.3(3)
O16-W4-O15	83.9(3)	O5-W8-O3	87.1(3)	O1-Cu1-O30	93.2(2)

Symmetry transformations used to generate equivalent atoms: #1 -x+1, -y+2, -z

Table S3. Selected bond lengths (Å) and angles (°) for **GeW₉-Co-SnR**

Bond	Length(Å)	Bond	Length(Å)	Bond	Length(Å)
W1-O29	1.740(16)	W5-O24	1.875(16)	W9-O22	1.930(14)
W1-O26	1.948(15)	W5-O28	1.950(16)	W9-O18	1.959(13)
W1-O33	1.961(15)	W5-O18	1.950(15)	W9-O15	1.960(17)
W1-O20	1.975(13)	W5-O1	1.964(14)	W9-O4	2.426(16)
W1-O28	1.978(17)	W5-O19	2.463(15)	Sn1-C1	2.10(3)

W1-O19	2.358(16)	W6-O9	1.754(17)	Sn1-O14	2.103(15)
W2-O12	1.753(15)	W6-O31	1.932(15)	Sn1-O16	2.108(15)
W2-O16	1.862(18)	W6-O15	1.935(18)	Sn1-O26#1	2.143(15)
W2-O6	1.971(14)	W6-O34	1.940(17)	Sn1-O25#1	2.156(14)
W2-O11	1.984(14)	W6-O1	1.960(13)	Sn1-O3	2.219(15)
W2-O32	2.029(16)	W6-O8	2.437(17)	Co1-O7	2.010(15)
W2-O4	2.347(15)	W7-O2	1.767(15)	Co1-O5#1	2.076(14)
W3-O27	1.733(18)	W7-O14	1.887(16)	Co1-O26#1	2.154(17)
W3-O25	1.938(15)	W7-O10	1.962(17)	Co1-O25	2.184(15)
W3-O21	1.949(13)	W7-O22	1.996(17)	Co1-O3#1	2.187(13)
W3-O20	1.960(13)	W7-O11	1.998(15)	Co1-O3	2.225(14)
W3-O34	1.984(16)	W7-O4	2.340(13)	Ge1-O4	1.750(15)
W3-O8	2.356(16)	W8-O13	1.753(15)	Ge1-O8	1.756(15)
W4-O23	1.758(14)	W8-O5	1.808(16)	Ge1-O19	1.762(13)
W4-O7	1.814(16)	W8-O6	1.936(15)	Ge1-O3	1.804(15)
W4-O10	1.932(19)	W8-O33	1.983(17)	C1-C2	1.522(10)
W4-O21	2.007(16)	W8-O24	2.070(16)	C2-C3	1.521(10)
W4-O31	2.029(18)	W8-O19	2.327(14)	C3-O35	1.27(4)
W4-O8	2.339(13)	W9-O17	1.746(18)	C3-O36	1.30(4)
W5-O30	1.728(18)	W9-O32	1.919(15)		
Bond	Angle(°)	Bond	Angle(°)	Bond	Angle(°)
O29-W1-O19	167.9(6)	O30-W5-O19	169.0(7)	O17-W9-O4	171.4(7)
O33-W1-O20	157.2(6)	O28-W5-O18	156.8(6)	O22-W9-O18	156.7(7)
O33-W1-O28	86.5(7)	O28-W5-O1	85.6(7)	O22-W9-O15	86.5(7)
O20-W1-O28	86.7(6)	O18-W5-O1	87.6(7)	O18-W9-O15	87.3(7)
O12-W2-O4	169.6(6)	O9-W6-O8	170.2(7)	O8-Ge1-O3	112.8(7)
O6-W2-O11	159.0(7)	O15-W6-O34	156.7(7)	O4-Ge1-O3	111.0(7)
O6-W2-O32	86.3(6)	O15-W6-O1	87.5(7)	O4-Ge1-O19	107.3(7)
O11-W2-O32	84.3(7)	O34-W6-O1	84.6(7)	O8-Ge1-O19	107.2(7)
O27-W3-O8	168.0(7)	O2-W7-O4	168.2(6)	C1-Sn1-O3	177.5(9)

O21-W3-O20	158.1(6)	O14-W7-O22	157.6(6)	O16-Sn1-O26#1	163.9(7)
O21-W3-O34	86.1(6)	O22-W7-O11	81.9(7)	C1-Sn1-O16	93.9(8)
O20-W3-O34	86.7(6)	O14-W7-O4	84.6(6)	O14-Sn1-O26#1	89.9(6)
O23-W4-O8	167.0(7)	O13-W8-O19	166.8(7)	O5#1-Co1-O3	170.3(6)
O10-W4-O21	157.8(6)	O6-W8-O33	158.6(6)	O7-Co1-O5#1	96.5(6)
O10-W4-O31	85.6(7)	O6-W8-O24	88.6(7)	O7-Co1-O25	94.3(6)
O21-W4-O31	81.9(7)	O33-W8-O24	81.0(7)	O25-Co1-O3#1	78.9(5)

Symmetry transformations used to generate equivalent atoms: #1 -x+1, -y+1, -z+1

Table S4. Hydrogen bonds for GeW₉-Cu-SnR

D-H...A	d(D-H)(Å)	d(H-A)(Å)	d(D-A)(Å)	∠(DHA) (°)
N1-H1A...O14	0.86	2.51	3.274(11)	148.3
N1-H1A...O27	0.86	2.58	3.272(13)	138.7
N1-H1B...O33	0.86	2.55	3.058(11)	119.1
N1-H1B...O2W#2	0.86	2.55	3.260(17)	139.9
N2-H2A...O17#3	0.86	2.50	3.305(12)	156.4
N2-H2B...O27	0.86	2.14	2.954(12)	157.5
N3-H3A...O15#3	0.86	2.30	3.097(12)	155.2
N3-H3B...O2W#2	0.86	2.14	2.952(16)	156.6
N4-H4A...O28#4	0.86	2.41	3.133(13)	142.6
N4-H4A...O22	0.86	2.54	3.049(14)	118.6
N4-H4B...O36#4	0.86	2.43	2.97(2)	121.7
N4-H4B...O13	0.86	2.57	3.328(14)	148.0
N5-H5A...O28#4	0.86	2.28	3.018(14)	143.5
N5-H5B...O3#5	0.86	2.01	2.850(13)	166.9
N6-H6A...O13	0.86	2.35	3.145(17)	153.3
N6-H6B...O19#5	0.86	2.29	3.046(16)	146.6
N7-H7A...O31#4	0.86	2.40	3.009(11)	128.2
N7-H7A...O20#6	0.86	2.58	3.305(11)	143.0
N7-H7B...O22	0.86	2.05	2.901(11)	171.0
N8-H8A...O25#2	0.86	2.29	3.110(11)	159.6

N8-H8B···O6	0.86	2.41	3.198(12)	152.6
N9-H9A···O9#4	0.86	2.32	3.118(12)	153.7
N9-H9B···O34#2	0.86	2.03	2.878(11)	170.7
N10-H10A···O32#7	0.86	2.09	2.918(12)	160.2
N10-H10B···O12#1	0.86	2.35	2.838(11)	116.5
N10-H10B···O18#1	0.86	2.49	3.246(12)	146.9
N11-H11A···O35#1	0.86	2.53	2.963(18)	112.3
N11-H11A···O18#1	0.86	2.60	3.329(13)	143.6
N11-H11B···O3W#8	0.86	2.23	3.01(2)	149.2
N12-H12A···O11#7	0.86	2.48	3.255(12)	150.8
N12-H12A···O32#7	0.86	2.55	3.257(13)	139.9
N12-H12B···O3W#8	0.86	2.28	3.040(19)	147.4
N12-H12B···O28#7	0.86	2.52	3.023(11)	118.3
N13-H13A···O2#6	0.86	2.06	2.909(12)	166.7
N13-H13B···O8#2	0.86	2.60	3.426(13)	160.6
N14-H14A···O29#6	0.86	2.40	3.185(12)	152.8
N14-H14B···O16	0.86	2.24	3.089(12)	171.9
N15-H15A···O24#2	0.86	2.22	3.006(13)	151.2
N15-H15B···O33	0.86	2.06	2.882(12)	159.8

Symmetry transformations used to generate equivalent atoms: #1 -x+1, -y+2, -z; #2 x-1/2, -y+3/2, z+1/2; #3 x-1, y, z; #4 -x+3/2, y-1/2, -z+1/2; #5 -x+1, -y+1, -z; #6 x+1/2, -y+3/2, z+1/2; #7 -x+2, -y+2, -z; #8 x+1/2, -y+3/2, z-1/2.

Table S5. Hydrogen bonds for GeW₉-Co-SnR

D-H···A	d(D-H)(Å)	d(H-A)(Å)	d(D-A)(Å)	∠(DHA) (°)
N1-H1C···O10#2	0.86	2.57	3.36(3)	153.3
N1-H1D···O2W	0.86	2.58	3.28(5)	139.3
N1-H1D···O2#2	0.86	2.68	3.14(3)	115.4
N2-H2C···O32	0.86	2.35	3.15(3)	154.7
N2-H2D···O2W	0.86	2.08	2.89(4)	158.2
N3-H3A···O23#2	0.86	2.15	2.96(3)	156.8
N3-H3B···O18	0.86	2.52	3.32(3)	155.0

N3-H3B···O32	0.86	2.66	3.39(2)	143.7
N4-H4A···O5#3	0.86	2.30	3.08(3)	149.7
N4-H4B···O33#4	0.86	2.05	2.91(2)	172.1
N5-H5A···O16#3	0.86	2.38	2.99(3)	128.2
N5-H5A···O5#3	0.86	2.67	3.35(3)	136.9
N5-H5A···O25#5	0.86	2.67	3.42(3)	146.1
N5-H5B···O17	0.86	2.07	2.93(3)	173.5
N6-H6A···O29#4	0.86	2.31	3.12(3)	157.8
N6-H6B···O22	0.86	2.43	3.22(3)	151.4
N7-H7A···O3W#6	0.86	2.20	2.96(5)	148.3
N7-H7A···O12	0.86	2.58	3.07(2)	117.2
N7-H7B···O6	0.86	2.56	3.34(3)	151.9
N7-H7B···O13	0.86	2.65	3.36(3)	139.7
N8-H8A···O3W#6	0.86	2.22	2.98(5)	147.5
N8-H8B···O36#2	0.86	2.48	2.97(4)	116.9
N9-H9A···O7#2	0.86	2.38	2.86(3)	116.4
N9-H9A···O14#2	0.86	2.55	3.31(2)	146.9
N9-H9B···O13	0.86	2.08	2.92(3)	164.9
N10-H10A···O11	0.86	2.32	3.18(3)	172.5
N10-H10B···O27#5	0.86	2.45	3.23(3)	151.0
N11-H11A···O2	0.86	2.06	2.90(4)	163.4
N11-H11B···O28#4	0.86	2.30	3.08(3)	151.0
N12-H12A···O21#5	0.86	2.11	2.96(3)	169.0
N12-H12B···O24#4	0.86	2.59	3.41(3)	159.4
N13-H13A···O12	0.86	2.31	3.04(3)	143.2
N13-H13B···O34#5	0.86	2.09	2.92(3)	162.4
N14-H14A···O30#6	0.86	2.33	3.15(4)	158.7
N14-H14B···O9#5	0.86	2.35	3.13(4)	150.6
N15-H15A···O12	0.86	2.38	3.10(3)	142.3
N15-H15A···O17#6	0.86	2.60	3.10(3)	119.0

N15-H15B···O35	0.86	2.41	3.09(4)	136.1
N15-H15B···O30#6	0.86	2.65	3.40(4)	145.9

Symmetry transformations used to generate equivalent atoms: #2 $x+1, y, z$; #3 $-x+1, y-1/2, -z+1/2$; #4 $x-1, -y+1/2, z-1/2$; #5 $x, -y+1/2, z-1/2$; #6 $-x+1, y+1/2, -z+1/2$.

Table S6. EIS and electrochemical parameters using different CEs.

	R_s [Ω]	R_{ct} [Ω]	Z_w [Ω]	ΔE_p [mV]
SWNT	13.50	0.855	0.855	538
SWNT/ GeW ₉	13.52	0.774	0.789	482
SWNT/ GeW ₉ Cu ₄	14.09	0.649	1.024	477
SWNT/ GeW ₉ -Co-SnR	15.16	0.411	0.685	461
SWNT/ GeW ₉ -Cu-SnR	14.87	0.293	0.727	455
Pt	17.39	1.992	0.946	470

Table S7. Photovoltaic parameters for the DSSCs based on SWNT/ SnR as the CE with N719 sensitizer and I₃⁻/I⁻-based mediator.

SWNT/ SnR							
	1	2	3	4	5	Average Values	Standard Deviation
J_{sc}	13.30	13.32	13.70	13.05	12.88	13.25	0.31
V_{oc}	627	628	625	620	616	623	5.07
FF	0.638	0.643	0.630	0.640	0.632	0.637	0.005
E_{ff}	5.32%	5.38%	5.41%	5.18%	5.02%	5.26%	0.16%

Table S8. Photovoltaic parameters for the DSSCs based on SWNT/ **GeW₉-Cu-SnR** as the CE with N719 sensitizer and I₃⁻/I⁻-based mediator.

SWNT/ GeW₉-Cu-SnR							
	1	2	3	4	5	Average Values	Standard Deviation
J_{sc}	15.78	15.72	15.67	15.80	15.40	15.67	0.16
V_{oc}	626	624	617	620	618	621	3.87
FF	0.646	0.661	0.641	0.646	0.653	0.649	0.008
E_{ff}	6.38%	6.48%	6.19%	6.32%	6.21%	6.32%	0.12%

Table S9. Photovoltaic parameters for the DSSCs based on SWNT/ **GeW₉-Co-SnR** as the CE with N719 sensitizer and I₃⁻/I⁻-based mediator.

SWNT/ GeW ₉ -Co-SnR							
	1	2	3	4	5	Average Values	Standard Deviation
J_{sc}	14.72	15.23	15.02	15.55	15.51	15.21	0.35
V_{oc}	636	629	610	616	609	620	12.0
FF	0.662	0.655	0.659	0.642	0.671	0.658	0.011
E_{ff}	6.20%	6.27%	6.03%	6.15%	6.34%	6.20%	0.12%

Table S10. Photovoltaic parameters for the DSSCs based on SWNT/ GeW₉-Cu₄ as the CE with N719 sensitizer and I₃⁻/I⁻-based mediator.

SWNT/ GeW ₉ -Cu ₄							
	1	2	3	4	5	Average Values	Standard Deviation
J_{sc}	14.73	14.03	13.99	14.23	14.10	14.22	0.30
V_{oc}	614	612	618	630	633	621	9.53
FF	0.647	0.667	0.681	0.661	0.653	0.662	0.013
E_{ff}	5.85%	5.73%	5.89%	5.93%	5.83%	5.85%	0.075%

Table S11. Photovoltaic parameters for the DSSCs based on SWNT/ GeW₉ as the CE with N719 sensitizer and I₃⁻/I⁻-based mediator.

SWNT/ GeW ₉							
	1	2	3	4	5	Average Values	Standard Deviation
J_{sc}	14.47	14.30	14.26	14.33	14.35	14.34	0.079
V_{oc}	587	604	577	581	593	588	10.62
FF	0.640	0.647	0.645	0.653	0.647	0.646	0.005
E_{ff}	5.44%	5.59%	5.31%	5.43%	5.50%	5.45%	0.10%

Table S12. Photovoltaic parameters for the DSSCs based on SWNT as the CE with N719

sensitizer and I₃⁻/I⁻-based mediator.

SWNT							
	1	2	3	4	5	Average Values	Standard Deviation
J_{sc}	13.96	13.28	13.91	13.59	13.48	13.64	0.29
V_{oc}	576	591	580	574	589	582	7.65
FF	0.627	0.624	0.623	0.635	0.626	0.627	0.005
E_{ff}	5.04%	4.90%	5.03%	4.96%	4.97%	4.98%	0.057%

Table S13. Photovoltaic parameters for the DSSCs based on Pt as the CE with N719 sensitizer and I₃⁻/I⁻-based mediator.

Pt							
	1	2	3	4	5	Average Values	Standard Deviation
J_{sc}	16.29	15.92	16.14	16.30	15.76	16.08	0.24
V_{oc}	675	687	685	669	683	680	7.56
FF	0.574	0.575	0.576	0.564	0.576	0.573	0.005
E_{ff}	6.31%	6.29%	6.37%	6.14%	6.21%	6.26%	0.090%

Table S14. Photovoltaic parameters for the DSSCs based on various CEs with Z907 sensitizer and a Co(III/II)-based mediator.

	V_{oc} , mV	J_{sc} , mA cm ⁻²	FF	E_{ff} , %
SWNT	598	9.21	0.499	2.75
SWNT/ GeW ₉ -Cu ₄	590	10.16	0.518	3.10
SWNT/ GeW₉-Cu-SnR	633	10.53	0.491	3.28
SWNT/ GeW₉-Co-SnR	612	9.61	0.650	3.82
Pt	639	11.58	0.610	4.52

Table S15. Photovoltaic parameters for the DSSCs based on SWNT/ **GeW₉-Co-SnR** as the CE

with Z907 sensitizer and a Co(III/II)-based mediator.

SWNT/ GeW ₉ -Co-SnR							
	1	2	3	4	5	Average Values	Standard Deviation
J_{sc}	10.29	9.78	9.61	9.77	9.75	9.84	0.26
V_{oc}	603	617	612	616	619	613	6.35
FF	0.592	0.604	0.650	0.650	0.648	0.629	0.028
E_{ff}	3.67%	3.64%	3.82%	3.90%	3.91%	3.79%	0.13%

Table S16. Photovoltaic parameters for the DSSCs based on SWNT/ GeW₉-Cu-SnR as the CE with Z907 sensitizer and a Co(III/II)-based mediator.

SWNT/ GeW ₉ -Cu-SnR							
	1	2	3	4	5	Average Values	Standard Deviation
J_{sc}	10.53	10.33	10.22	10.26	10.28	10.32	0.12
V_{oc}	633	614	603	611	615	615	11.0
FF	0.491	0.546	0.550	0.506	0.514	0.521	0.026
E_{ff}	3.28%	3.46%	3.39%	3.17%	3.25%	3.31%	0.11%

Table S17. Photovoltaic parameters for the DSSCs based on SWNT/ GeW₉-Cu₄ as the CE with Z907 sensitizer and a Co(III/II)-based mediator.

SWNT/ GeW ₉ -Cu ₄							
	1	2	3	4	5	Average Values	Standard Deviation
J_{sc}	10.95	10.34	10.16	10.39	10.45	10.46	0.30
V_{oc}	584	590	590	590	601	591	6.16
FF	0.503	0.519	0.518	0.487	0.493	0.504	0.014
E_{ff}	3.21%	3.17%	3.10%	2.98%	3.10%	3.11%	0.087%

Table S18. Photovoltaic parameters for the DSSCs based on SWNT as the CE with Z907 sensitizer and a Co(III/II)-based mediator.

SWNT							
	1	2	3	4	5	Average Values	Standard Deviation
J_{sc}	9.21	9.05	9.46	9.88	9.78	9.48	0.36
V_{oc}	598	590	586	602	596	594	6.39
FF	0.499	0.495	0.514	0.462	0.462	0.486	0.023
E_{ff}	2.75%	2.64%	2.85%	2.75%	2.70%	2.74%	0.077%

Table S19. Photovoltaic parameters for the DSSCs based on Pt as the CE with Z907 sensitizer and

a Co(III/II)-based mediator.

	Pt						
	1	2	3	4	5	Average Values	Standard Deviation
J_{sc}	11.58	11.45	11.75	11.54	11.78	11.62	0.14
V_{oc}	639	637	640	641	642	640	1.92
FF	0.610	0.600	0.617	0.618	0.611	0.611	0.007
E_{ff}	4.52%	4.35%	4.64%	4.57%	4.62%	4.54%	0.12%

References:

S1 U. Kortz, S. Nellutla, A. C. Stowe, N. S. Dalal, U. Rauwald, W. Danquah and D. Ravot, *Inorg. Chem.*, 2004, **43**, 2308-2317.

S2 G. M. Sheldrick, *SHELXL97, Program for Crystal Structure Refinement*, University of Göttingen: Göttingen, Germany, 1997; G. M. Sheldrick, *SHELXS97, Program for Crystal Structure Solution*, University of Göttingen: Göttingen, Germany, 1997.

S3 U. O. Krašoves, M. Berginc, M. Hočevar and M. Topič, *Sol. Energy Mater. Sol. Cells*, 2009, **93**, 379-381.